HHS Public Access

Author manuscript

ACS Nano. Author manuscript; available in PMC 2018 July 25.

Published in final edited form as:

ACS Nano. 2017 July 25; 11(7): 6691–6702. doi:10.1021/acsnano.7b00824.

Microfluidics Enabled Bottom-Up Engineering of 3D Vascularized Tumor for Drug Discovery

Pranay Agarwal[1,2,#], **Hai Wang**[1,2,3,#], **Mingrui Sun**[1,2], **Jiangsheng Xu**[1,2,3], **Shuting Zhao**[1,2], **Zhenguo Liu**[2,4], **Keith J. Gooch**[1,2], **Yi Zhao**[1], **Xiongbin Lu**[5], and **Xiaoming He**[1,2,3,*]

[1]Department of Biomedical Engineering, The Ohio State University, Columbus, OH 43210, USA

[2]Dorothy M. Davis Heart and Lung Research Institute, The Ohio State University, Columbus, OH 43210, USA

[3]Comprehensive Cancer Center, The Ohio State University, Columbus, OH 43210, USA

[4]Division of Cardiovascular Medicine, The Ohio State University, Columbus, OH 43210, USA

[5]Department of Cancer Biology, The University of Texas MD Anderson Cancer Center, Houston, TX 77030, USA

Abstract

Development of high-fidelity 3D models to recapitulate the tumor microenvironment is essential for studying tumor biology and discovering anticancer drugs. Here we report a method to engineer the 3D microenvironment of human tumor, by encapsulating cancer cells in the core of microcapsules with a hydrogel shell for miniaturized 3D culture to obtain avascular microtumors first. The microtumors are then used as the building blocks for assembling with endothelial cells and other stromal cells to create macroscale 3D vascularized tumor. Cells in the engineered 3D microenvironment can yield significantly larger tumors *in vivo* than 2D-cultured cancer cells. Furthermore, the 3D vascularized tumors are 4.7 and 139.5 times more resistant to doxorubicin hydrochloride (a commonly used chemotherapy drug) than avascular microtumors and 2D-cultured cancer cells, respectively. Moreover, this high drug resistance of the 3D vascularized tumors can be overcome by using nanoparticle-mediated drug delivery. The high-fidelity 3D tumor

*Correspondence should be addressed to: Xiaoming He, Ph.D., Department of Biomedical Engineering, The Ohio State University, 1080 Carmack Road, Columbus, OH, Phone: 1 (614) 247-8759, Fax: 1 (614) 292-7301, he.429@osu.edu.
#Contributed equally

Supporting information

Microfluidic encapsulation device. Microfluidic perfusion device. Rheological data of core extracellular matrices. Proliferation of human MCF-7 cancer cells in different core ECMs. Viability of sample in the microfluidic perfusion device without perfusion. ELISA data of vascular endothelial growth factor (VEGF). Blood vessel formation in the microfluidic perfusion device. Shrinkage of the mixture of three types of single cells in collagen hydrogel under dynamic and static culture. No evident interconnected network of blood vessels formed in four days under the conventional static culture. Immunostaining analysis of vascularization in the microfluidic perfusion device with CD31. Immunostaining analysis of vascularization in the microfluidic perfusion device with VE-CADHERIN. Drug responses of 2D-cultured cells. Distribution of doxorubicin in 2D-cultured cells, 3D avascular μtumor, and 3D vascularized tumor. Expression of CD44 and CD24 on 2D-cultured cancer cells, 3D avascular μtumors, and the μtumors in 3D vascularized tumor. Morphology of the nanoparticles used in this study. List of primers used for gene expression studies.

Notes

The authors declare no competing financial interest. We thank Deepti Gupta for her technical assistance during the course of this project.

model may be valuable for studying the effect of microenvironment on tumor progression, invasion, and metastasis, and for developing effective therapeutic strategy to fight against cancer.

Graphical abstract

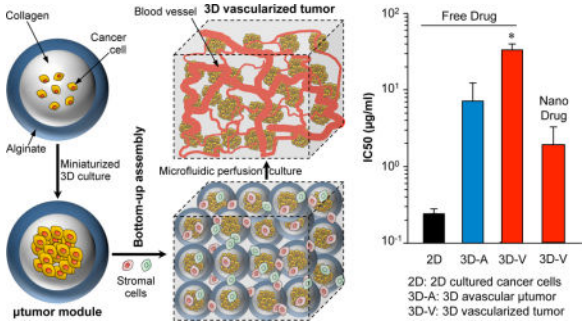

Keywords

vascularization; vasculogenesis; angiogenesis; core-shell microcapsule; tumor microenvironment

Cancer is one of the major causes of death globally.[1,2] However, development of new anticancer drugs are slow, expensive, and most of them provide little improvement in quality or extension of life even though they may work well in animal models.[3] The latter is due to the huge interspecies differences in cell, tissue, and organ physiology and anatomy.[4–6] On the other hand, the most commonly used 2D culture method of preparing cancer cells for drug discovery has proven to induce altered gene and protein expression in cells compared to 3D culture that is natural to nearly all cells in human body.[7–9] Current approaches for 3D culture include suspending cells in liquid medium to form multicellular spheroids and seeding cells in hydrogels or porous scaffolds.[10–14] Although they are simple and inexpensive, it is difficult to achieve high-throughput production and obtain spheroids of uniform size.[10,11] Moreover, the lack of vascularization is a critical limitation of most contemporary 3D tumor models for drug discovery, because the diffusion limit (typically less than ~200 μm, the half distance between two blood capillaries)[11,15–18] of nutrients and oxygen in highly cellularized tissue (such as tumor) may result in viable cells only in the surface layer of less than ~200 μm in the tumor model. Vascularization is also required for studying cancer metastasis *in vitro*, and the difference between normal vasculature and that in solid tumors (immature, tortuous, and hyperpermeable vessels) offers an opportunity for anticancer therapies.[19–21] Moreover, stromal cells including endothelial cells may impact the cancer cells *via* paracrine factors and modification of the extracellular matrix,[22–28] which may affect the sensitivity of cancer cells to anticancer drugs. Therefore, tumor vasculature is an important component of the tumor microenvironment that must be incorporated in 3D tumor models for high-fidelity drug discovery and understanding of tumorigenesis and metastasis. However, contemporary work on vascularization *in vitro* has been focused on random assembly of endothelial cells in a homogeneous system (*e.g.*, hydrogel) to form new blood vessels (*i.e.*, vasculogenesis) with no control on their distribution; vasculogenesis around a bioprinted or microfabricated track or channel that may be simple in geometry or difficult to be embedded with interstitial cancer cells; and the sprouting of existing vessels to

produce new capillaries (*i.e.*, angiogenesis).[29–42] Lastly, the effect of vascularization on cancer drug resistance *in vitro* has not been well studied.

In this study, we developed a "bottom-up" approach to fabricate 3D vascularized human tumor with controlled formation of a complex 3D vascular network and studied the effect of vascularization on cancer drug resistance. This is achieved by first encapsulating and culturing cancer cells in core-shell microcapsules (< ~200 μm in radius) consisting of a type-I collagen rich core enclosed in a semipermeable alginate hydrogel shell to form cell aggregates or micro-tumors (μtumors), using a high-throughput non-planar polydimethylsiloxane (PDMS) microfluidic encapsulation device (Scheme 1a and Figure S1). Next, these μtumors in core-shell microcapsules are used as the building blocks to assemble with stromal cells (including endothelial cells) in a collagen hydrogel under dynamic perfusion culture in a PDMS-glass microfluidic perfusion device, to form millimeter-sized 3D vascularized tumor (Scheme 1b and Figure S2). It is hypothesized that assembling microscale (less than the diffusion limit of nutrients and oxygen in cellularized tissue) cell-containing modules will provide geometric and physicochemical guidance to the vascular cells, thereby enabling the formation of a complex 3D vascular network around the cancer cells in the modules to mimic the vascular and cellular configuration in *in vivo* tumors. As tumor-associated stromal cells have been shown to contribute to cancer drug resistance,[43,44] we further examined the response to free and nanoparticle-encapsulated drug of the 3D vascularized tumor compared to conventional 3D avascular μtumors and 2D-cultured cells.

RESULTS AND DISCUSSION

Fabrication and characterization of avascular μtumors

Figure 1a shows the spherical and core-shell morphology of the microcapsules together with the fibrous collagen core revealed by scanning electron microscopy (SEM). The microcapsules have a total and core size (in diameter) of 387 ± 15 μm and 273 ± 21 μm, respectively (Figure 1b). Since the diffusion limit for oxygen and nutrients *in vivo* is less than ~200 μm, the small size (less than ~200 μm in radius) of the core-shell microcapsules allows adequate mass transport for all the encapsulated cells to survive and proliferate. By suspending MCF-7 human mammary cancer cells at 5×10^6 cells/ml in the core collagen solution (1.5 mg/ml and introduced into the microfluidic encapsulation device *via* I3, Scheme 1a and Figure S1a), 33 ± 6 cells can be encapsulated in the core of each resultant microcapsule (Figure 1b). Figure 1c shows the morphology and proliferation of the MCF-7 cells encapsulated and cultured in the microcapsules: Over 10 days under the miniaturized 3D culture, the cells proliferated to form highly viable μtumors (*i.e.*, avascular aggregates of cancer cells) with 1442 ± 317 in each μtumor. The high viability is probably due to the small size of the μtumors (less than ~150 μm in radius) that is less than the diffusion limit of oxygen and nutrients (~200 μm in highly cellularized tissue).[11,15–18] It is worth noting that the cell proliferation over 10 days inside the microcapsules does not have significant impact on the overall size of the microcapsules.

We next investigated the effects of culturing microenvironment on the growth and metastatic potential of the encapsulated cancer cells, by varying the collagen density in the core of the

microcapsules from 0.5 to 3 mg/ml, to modulate the physicochemical properties (*i.e.*, stiffness and cell adhesion) of the core extracellular matrix (ECM) in the microcapsules. In order to further increase the mechanical property to study the role of stiffness alone on the cell proliferation, we added 1–2% (w/v) of alginate together with collagen to make the core ECM in some cases because alginate has no adhesion domain for cells to attach. Rheological analyses show that the elastic modulus (G′) can be tuned over ~1–15000 Pa (Figures 1d and S3), spanning the range of stiffness of normal and malignant mammary tissues.[45–47] With 3 mg/ml collagen in the core ECM (G′ = 22 Pa), we observed small and multiple aggregates in the core-shell microcapsules after 10 days of culture (Figure S4). When the collagen concentration is lowered to 1.5 mg/ml (G′=3.68 Pa) or 0.5 mg/ml (G′=0.48 Pa), the cell proliferation is significantly improved (by 5.9 and 4.6 folds for 1.5 and 0.5 mg/ml, respectively) compared to that of 3 mg/ml (Figures 1e and S4). To determine the role of stiffness alone on the cell proliferation, we included alginate (1–2%) in the 1.5 mg/ml collagen core ECM. As shown in Figures 1e and S4, further increasing the stiffness with alginate significantly reduced the MCF-7 cell proliferation in the core-shell microcapsules.

Malignant transformation of tumors of epithelial origin including the mammary adenocarcinoma is often accompanied by changes in the tumor microenvironment including the ECM stiffness.[46,48] Therefore, we investigated the effect of the ECM stiffness on the malignant behavior of MCF-7 cells under the miniaturized 3D culture by examining the expression of two epithelial to mesenchymal transition (EMT) marker genes including *VIMENTIN* and *CXCR4* and one epithelial marker gene (*E-CADHERIN*). As the stiffness of the ECM is increased (keeping the cell adhesion constant by using the same collagen density of 1.5 mg/ml), we observed significantly increased expression of *VIMENTIN* (by up to 10 folds) and *CXCR4* (by up to 3.6 folds) without significant change in the expression of *E-CADHERIN* (Figure 1f). These data suggest the ECM stiffness is a crucial regulator of EMT under the miniaturized 3D culture, which is consistent with previous reports regarding the effect of stiffness on the EMT of cancer cells cultured under 2D and bulk 3D conditions.[45,48,49] Taken together, these data show the capability of engineering the tumor microenvironment within the core-shell microcapsules to study the biological behavior of cancer cells under miniaturized 3D culture, including interrogating the contribution of environmental cues to tumor progression and metastatic potential.

Fabrication and characterization of vascularized 3D tumors

After successful formation of μtumors in the core-shell microcapsules, we assembled them in a PDMS-glass microfluidic perfusion device with stromal cells for perfused culture to form 3D vascularized tumor. A schematic overview and real images of the microfluidic perfusion device are shown in Scheme 1b and Figure S2. The device consists of a sample chamber (width × length × depth = 1 × 5 × 0.5 mm) connected to two reservoirs of culture medium through eight micro-pillars (width × length × depth: 0.8 × 0.8 × 0.5 mm). The perfusion (with the medium of HUVECs) is driven by hydrostatic pressure (ΔP) resulting from the difference in height (Δh) of the medium column linked to the two reservoirs on the two different sides of the sample (Scheme 1b and Figure S2). The composite hydrogel consisting of encapsulated μtumor modules together with primary human umbilical vein endothelial cells (HUVECs) and human adipose-derived stem cells (hADSCs) in 1.5 mg/ml

type-I collagen was injected into the sample chamber (~10 μl) of the microfluidic perfusion device. The hADSCs are incorporated in the system because they are present in breast tumor stroma *in vivo*,[50] and can positively influence the vascularization by secreting pro-angiogenic growth factors.[51,52] After gelling at 37 °C for 30 min, the composite hydrogel is constrained within the sample chamber of the microfluidic device by the eight micro-pillars. A total of ~50 core-shell microcapsules encapsulated with μtumors could be placed in the sample chamber. We monitored the effect of perfusion on the viability and growth of the assembled μtumors and stromal cells. Without perfusion (achieved by adding the same amount of medium on both sides of the sample chamber so that Δh was 0), capillary formation was minimal and many cells were dead by day 4 (Figure S5). When perfusion was applied through an initial hydrostatic pressure of 1 cm (Δh) of medium (ΔP: ~100 Pa) with medium being changed every 12 hr before Δh approached 0 (Figure S2d–e), both the cancer and stromal cells were highly viable (Figure 2a) and vascular structures could be observed after 4 days of culture (condition 1 in Figure 2b). This is probably because the radius of the building blocks (*i.e.*, μtumors in core-shell microcapsules) is less than the diffusion limit of nutrients and oxygen in highly cellularized tissue (~200 μm),[11,15–18] which enables adequate transport of nutrients and oxygen to all cells in the system including cells in the core of the μtumors. Therefore, all further experiments were conducted under dynamic culture with the hydrostatically driven perfusion.

Next, we investigated the effect of the presence of the 3D building blocks or modules (*i.e.*, μtumors in core-shell microcapsules) on guiding the endothelial cells in the collagen hydrogel for capillary morphogenesis around the encapsulated μtumors. Cancer cells in the μtumors should release cytokines such as VEGF, bFGF, and IL-8 to promote vasculogenesis and angiogenesis.[53] To confirm this, the concentration of VEGF (that has a larger molecular weight than bFGF and IL-8) in the 1 ml of medium for culturing the same number (20,000) of encapsulated cells (in μtumors) and 2D-cultured cancer cells at different days was quantified by using enzyme-linked immunosorbent assay (ELISA). As shown in Figure S6, VEGF indeed can be released through the alginate shell of the microcapsules into medium and the VEGF produced by cells in the encapsulated 3D μtumors is significantly more than that of 2D cultured cells during the first 3 days. In addition, the μtumors or core-shell microcapsules should provide a geometric guidance for the endothelial cells to assemble and form a complex 3D vascular network around the building blocks.[34,54] Indeed, after one-day culture, HUVECs displayed elongated morphology around the microcapsules. Controlled formation of vacuoles and tube-like structures around the microcapsules was observed on day 2. On day 4, controlled formation of a complex 3D capillary network around the microcapsules was observable throughout the sample (condition 1 in Figures 2b–c and S7).

Because microcapsules act as a physical barrier to prevent direct cell-cell contact between the encapsulated μtumors and HUVECs, contribution of the μtumors to vasculogenesis is through the secretion of vasculogenic factors by cells in the μtumors. We found that vasculogenic morphogenesis of HUVECs is highly dependent on the co-culture with the μtumors, since the formation of interconnected vascular networks is minimal in the absence of μtumors (*i.e.*, mixed with empty microcapsules) within 4 days of culture with perfusion (condition 2 in Figures 2b–c and S7). We further investigated the effect of direct cell-cell contact between the μtumors and HUVECs on vascularization in addition to the

aforementioned cytokine effect. For this, we dissolved the alginate shell of the core-shell microcapsules by perfusing the samples with 75 mM sodium citrate for 5 min after one day of culture. During the course of the following three days of perfusion culture with medium, we observed significantly enhanced vascularization (condition 3 in Figures 2b–c and S7). However, vascularization could not be achieved if the same numbers of the three types of single cells (*i.e.*, without any microencapsulation or μtumors) were mixed in collagen for loading into the chamber to make the samples. As shown in Figure S8a, The samples were observed to shrink greatly and adhere only onto the surface of the micro-pillars in the sample chamber on days 1–4, and no clear network of blood vessels could be observed in the device. Similar phenomenon of apparent shrinkage (by ~3 times in diameter or ~27 times in volume in 4 days) was also observed with the conventional method of directly mixing the three types of cells (without any microencapsulation) in collagen hydrogel for static culture in 24-well plates (Figure S8b). Importantly, the presence of encapsulated μtumors (even if the alginate hydrogel shell is dissolved after 1-day culture) can prevent this issue (Figures 2, S7, and S8b). In order to confirm the advantage of using both microencapsulation and microfluidic perfusion device, vascularization was further examined in the samples under conventional static culture in 24-well plates. As shown in Figure S9, few HUVECs stayed the collagen hydrogel after 1-day culture for the samples without microencapsulation under static culture, possibly due to the significant shrinkage of the samples. Although HUVECs could be observed in the groups with encapsulated μtumors (without or with dissolution of alginate after 1-day culture), the cells did not form an interconnected vascular network in four days as they did under dynamic perfusion culture in the microfluidic perfusion devices (Figure 2c).

To further confirm that the vasculature engineered using the μtumors with dissolution of the alginate hydrogel shell after one-day culture, we examined it for its 3D structural integrity and the presence of characteristic CD31 and VE-CADHERIN protein markers. Immunofluorescent staining of these markers together with F-ACTIN cytoskeleton filaments shows the formation of a complex microvascular network with good interconnectedness after 4-day culture in the microfluidic perfusion device (Figures 2d and S10–S11, and Movie S1). Moreover, we observed the presence of lumens in the vessels enclosed by HUVECs as shown in the bottom panels in Figures 2d and S10–S11.

In vivo tumorigenicity of the μtumors and stromal cells

To understand *in vivo* tumorigenesis of the 3D-engineered system of μtumors mixed with HUVECs and hADSCs in collagen, we injected it subcutaneously into athymic nude mice that were sacrificed at 14 days after injection to obtain the resultant tumors. Control experiments with 2D-cultured MCF-7 cancer cells alone and a mixture of single hADSCs, HUVEC and MCF-7 cells (at the same ratio as that in the 3D-engineered system) without any microencapsulation were performed in parallel. The total number of cells were the same for all the conditions. As shown in Figure 3a–b, the 3D-engineered system (conditions 3 and 4) is much more tumorigenic than the cancer cells alone (condition 1) or mixture of hADSCs, HUVEC and MCF-7 cells (condition 2). Although the difference between the groups without (condition 3) and with (condition 4) alginate dissolution at one day after injection is insignificant, the size/weight is more uniform for the tumors obtained under

condition 4 than 3 (Figure 3a–b). To find out if the difference in size of the tumors formed under the four different conditions could be related to their difference in vascularity, we quantified the density of blood vessels in the tumors. The density of blood vessels (containing red blood cells or RBCs indicated by arrow heads) in the tumors formed with the 3D-engineered system (conditions 3 and 4) is significantly higher than that formed from conditions 1 and 2 (Figure 3c–d). The staining of human CD31 (hCD31) shows that blood vessels of human origin are readily observable only for conditions 4 and 3 and green fluorescence is barely observable in the tumors for condition 2 (Figure 3e). The average size of blood vessels is also larger in the tumors formed from the engineered system than 2D cultured cells (Figure 3c). It is worth noting that no microcapsules were observed in the tumors under condition 3, indicating the alginate hydrogel shell of the microcapsules was liquefied/degraded during the 14 days *in vivo*. Taken together, these data suggest that 3D culture of MCF-7 cells and incorporation of supporting HUVECs and hADSCs can improve *in vivo* tumorigenicity compared to the conventionally 2D-cultured cells.

Drug discovery with the 3D vascularized tumors

After successful fabrication and characterization of the avascular 3D μtumors and *in vitro* vascularized 3D tumors, we analyzed their responsiveness to chemotherapy to illustrate their utility for drug discovery. The Food and Drug Administration (FDA) approved anticancer drug doxorubicin hydrochloride (DOX) for treating breast cancer was used.[55] We compared the cytotoxicity of DOX on the conventionally 2D-cultured MCF-7 cancer cells, avascular 3D μtumors, and *in vitro* vascularized 3D tumors. DOX was administered by incubating it with the three different model systems for 4 days at concentrations ranging from 0–100 μg/ml. The CCK-8 cell viability assay was used to assess the cell viability. As shown in Figure 4a, 2D-cultured MCF-7 cells were the most sensitive to DOX. Cancer cells in the engineered 3D (avascular) μtumors (3D-A) were significantly more resistant to the free DOX than the 2D-cultured cells. Moreover, cells in the vascularized 3D tumors (3D-V, cultured with perfusion) are significantly more resistant to the free DOX from 10–60 μg/ml than the cancer cells in the 3D avascular μtumors. The inhibition concentration of free DOX to kill 50% of cells (IC_{50}) was 0.24, 7.13 (increased by 29.7 times), and 33.48 (increased by 139.5 times) μg/ml on average for the 2D-cultured cells, cells in the avascular 3D μtumors, and all the three types of cells in the vascularized 3D tumors, respectively. The IC50 of cells in the vascularized 3D tumors is 4.7 times of that of cells in the avascular 3D μtumors.

It is worth noting that the high drug resistance of the vascularized 3D tumors is not due to the possible high drug resistance of HUVECs or hADSCs. In fact, MCF-7 cancer cells (IC50: 0.24 μg/ml, Figure 4a) are more drug resistant than hADSCs (IC50: 0.17 μg/ml, Figure S12a) and HUVECs (IC50: 0.09 μg/ml, Figure S12b). Although the mixture of the three types of cells (hADSCs+HUVECs+MCF-7 cells, IC50: 0.75 μg/ml, Figure S12c) is more drug resistant than any of the three types cells alone, it is much less drug resistant than the vascularized 3D tumors (3D-V, IC50: 33.48μg/ml, Figure 4a). The differential drug sensitivity may not be attributed to the difference in DOX availability either, as the DOX is observed to homogeneously distribute in all the cells under all the three different culture conditions (Figure S13). To investigate more on the possible mechanisms of drug resistance of the 3D-cultured MCF-7 cells in the avascular μtumors and vascularized tumors, we

studied the expression of the putative mammary cancer stem cell (CSC) marker CD44 together with the differentiation marker CD24 using immunocytochemistry and flow cytometry.[55] As shown in Figure S14, the expression of CD24 decreases significantly and the expression of CD44 is significantly increased in the avascular 3D μtumor cells, compared to the 2D-cultured cancer cells. Similar trends in the expression of CD24 and CD44 are observed for the 3D μtumors embedded in the 3D vascularized tumor compared to the 2D-cultured cancer cells (Figure S14a). Therefore, the mechanisms associated with the CSC drug resistance[55–59] may contribute to the enhanced IC_{50} of cells in the 3D μtumors. Furthermore, we propose that there should be interplay among various factors (intracellular changes, paracrine signaling, and modification of the ECM)[22–26] that may contribute to the reduced drug sensitivity in the avascular 3D μtumors and *in vitro* vascularized 3D tumors, which warrants further investigation.

To show the utility of our 3D vascularized tumor model for anticancer drug discovery, we tested the efficacy of a nanoparticle-mediated combination therapy using the models. As schematically illustrated in Figure 4b, the LC60S-DI nanoparticles used are composed of a lipid (L) outer membrane and a fullerene (C60) core embedded in a matrix of mesoporous silica (S), and encapsulated with DOX (D) and indocyanine green (ICG or I).[60] The nanoparticles are ~60 nm in diameter with a round morphology (Figure 4c and Figure S15) and have a negatively charged surface as indicated by the negative surface zeta potential of approximately −22.3 mV (Figure 4d). The former is excellent for cellular uptake and passive targeting of tumor *in vivo* while the latter is important for the blood stability of the nanoparticles.[19–21,60] The nanoparticles enable combined chemo, photothermal, and photodynamic therapies for tumor destruction, because the encapsulated ICG can efficiently absorb near infrared (NIR, 800 nm) laser to generate heat and reactive oxygen species.[60] Moreover, release of the encapsulated DOX can be precisely controlled by dosing the NIR irradiation. To check the anticancer capability of the LC60S-DI nanoparticles on the most drug-resistant 3D vascularized tumors, we perfused/incubated the tumors in the microfluidic perfusion device with the nanoparticles for 12 hr, irradiated the tumors with NIR (at 1.5 W/cm^2 for 1 min), and further cultured them for 3.5 days with a total treatment time of 4 days. As shown in Figure 4e, the LC60S-DI nanoparticle-mediated combination therapy is significantly more effective than chemotherapy with free DOX alone for destroying the 3D vascularized tumors. The cell viability at the DOX dose of 10 μg/ml in nanoparticles is significantly lower than that of chemotherapy with 10 μg/ml in free DOX. The IC_{50} significantly dropped by more than 16 times to ~1.9 μg/ml with the combination therapy compared to chemotherapy with free DOX (Figure 4f). It has been reported that a dose of 2.5 mg/kg (body weight) for DOX encapsulated in the nanoparticles could result in effective destruction of tumors *in vivo* while the same dose of free DOX has minimal impact on tumor growth. If the density of mammalian tissue is assumed to be ~1 kg/l (*i.e.*, the density of water), the 2.5 mg/kg(body weight) is equivalent to 2.5 mg/l or 2.5 μg/ml. Consistent with the *in vivo* studies, our data show that 2.5 μg/ml of DOX in the nanoparticles could effectively kill the 3D vascularized tumor (Figure 4e–f), while 2.5 μg/ml of free DOX has minimal impact on the survival of the 3D vascularized tumor although it is effective in killing 2D-cultured cancer cells and 3D avascular μtumors (Figure 4a). Therefore, our *in vitro* 3D vascularized tumor model may be valuable for replacing conventional animal

models and 2D-cultured cancer cells and 3D avascular μtumors, to prioritize candidate anticancer compounds for further confirmation with clinical trial studies.

CONCLUSIONS

In summary, we demonstrate the ability to form μtumor modules in core-shell microcapsules using a high-throughput non-planar microfluidic encapsulation technology. The physicochemical properties of the core-shell microcapsules can be readily modulated to study their effects on the proliferation and gene expression of the encapsulated cancer cells. Using the μtumors as the building blocks and geometric guidance of vasculogenesis, we fabricated 3D vascularized human mammary tumor from bottom up by assembling the μtumors with stromal cells including endothelial cells and adipose-derived stem cells. We confirmed the tumor vasculature based on vessel structures and protein markers. We further tested the anticancer efficacy of free DOX and DOX encapsulated in nanoparticles (LC60S-DI) with the *in vitro* vascularized 3D human tumors. The results support the importance of tumor microenvironment on the effectiveness of chemotherapy. This *in vitro* vascularized 3D human tumor model may be valuable for studying the role of the tumor microenvironment including cell-cell and cell-ECM interactions in cancer progression and metastasis and for drug discovery.

MATERIALS AND METHODS

Materials

Polydimethylsiloxane (PDMS, Sylgard 184) was purchased from Dow Corning (Midland, MI, USA). SU8 2100 and 2025 were purchased from MicroChem (Westborough, MA, USA). Fetal bovine serum (FBS) was purchased from Invitrogen (Carlsbad, CA, USA). MCF-7 human mammary cancer cells were purchased from ATCC (Manassas, VA, USA). Primary human umbilical vascular endothelial cells (HUVECs) with and without green fluorescence protein (GFP) were purchased from Angio-Proteomie (Boston, MA, USA) and Lonza (Allendale, NJ, USA), respectively. Primary human adipose-derived stem cells (hADSCs) were purchased from Lonza (Allendale, NJ, USA). The rat-tail type I collagen was purchased from BD Bioscience (Franklin Lakes, NJ, USA). Doxorubicin hydrochloride (DOX) was purchased from LC laboratories (Woburn, MA, USA). The phospholipid 1,2-dihexadecanoyl-sn-glycero-3-phosphocholine (DPPC) was purchased from Anatrace (Maumee, OH, USA). All other materials were purchased from Sigma (St. Louis, MO, USA) unless specifically noted otherwise.

Fabrication of microfluidic encapsulation device

To fabricate the non-planar microfluidic cell encapsulation device, microchannels were patterned on a silicon wafer by multilayer photolithography technique. A 100 μm of a layer of SU8 2025 was first coated and then soft-baked followed by exposure to ultraviolet (UV) light through the first shadow mask (Cad/Art services, Bandon, OR, USA) printed with the core channel. After a post-exposure baking, an additional layer (50 μm) of SU-8 photoresist was spun coated, soft baked, exposed with a second shadow mask to pattern the shell channel. The third layer for oil/separation channel was similarly patterned. All three

exposures were aligned using an EVG620 automated mask aligner. In the end, the SU8 pattern on the substrate was developed in the SU-8 developer (MicroChem), rinsed with isopropyl alcohol, and dried using nitrogen gas. The microfluidic encapsulation devices were then made by replica molding of PDMS. The mixture of cross-linker and PDMS pre-polymer (1:10) was poured on a patterned silicon wafer. PDMS was cured at 65 °C for at least 3 hr and then carefully peeled off. Two PDMS slabs with the same channel design were then plasma-treated for 30 s using a Harrick (Ithaca, NY, USA) PDC-32G plasma cleaner at 18 W and 27 Pa, wetted with methanol, aligned and bonded together under a microscope to produce the final cell encapsulation device. Assembled device was kept on a hotplate at 80 °C for ~ 10 min to evaporate residual methanol and further kept at 65 °C for 2 days to make it sufficiently hydrophobic for experiments.

Fabrication of microfluidic perfusion device

The microfluidic perfusion device was composed of a top PDMS part, a bottom PDMS part, and a bottom glass slide (Figure S2). The top PDMS part (12 mm in thickness) was prepared by using 60-mm petri dish as the mold and punched with four holes (1–4) using a standard 9.5 mm biopsy puncher (Figure S2a). To fabricate the bottom PDMS part, two layers of SU8 2100 were spun-coated on a silicon wafer to achieve a total thickness of 500 μm. After soft baking, wafer was exposed to UV light through the shadow mask (with features including micro-pillars, sample chamber, and reservoirs, Figure S2b), followed by post-exposure baking and development. The PDMS pre-polymer mixed with cross-linker was poured on the wafer and baked at 65 °C for at least 3 hr. The bottom PDMS part (2 mm in thickness) was then carefully peeled off from the wafer without damaging the pillars. Thereafter, four holes (1–4) were punched in the bottom PDMS part using a standard 2 mm biopsy puncher (Figure S2b). The bottom and top PDMS parts were then plasma-treated, the four holes aligned, and the two parts bonded together with the features (*i.e.*, micro-pillars, sample chamber, and reservoir) on the external surface of the resultant PDMS assembly. The PDMS assembly was autoclaved before further use. After loading sample in the sample chamber, the PDMS assembly was bond to a thin (0.15 mm in thickness) glass slide (Fisher Scientific, Waltham, MA, USA) to form the final PDMS-glass microfluidic perfusion device as shown in Figure S2c. It is worth noting that any potential wetting of the surface of the PDMS assembly during and after loading sample in the chamber could weaken the binding between the assembly and glass slide. This issue was minimized by designing the device with a total binding area between the PDMS assembly and glass slide being much bigger than the area of the sample chamber as shown in Fig. S2b. In addition, the two parts were bonded immediately after loading sample in the chamber to minimize the time of possible surface wetting.

Cell culture

MCF-7 cancer cells were cultured in EMEM (base medium, ATCC) supplemented with 10% FBS, 10 μg/ml insulin, 100 U/ml penicillin, and 100 μg/ml streptomycin. HUVECs with or without GFP were cultured on gelatin-coated flask in endothelial basal medium (EBM, Lonza) supplemented with an EGM-2 bullet kit (Lonza). The hADSCs were cultured in hADSC basal medium (Lonza) supplemented with 10% FBS, 2 mM of L-glutamine, and 50 μg/ml of gentamicin amphotericin. All cells were cultured at 37 °C in humidified 5% CO_2

incubator. The medium was changed every other day. HUVECs and hADSCs between 3–7 passages were used. Samples in the microfluidic perfusion device were perfused with the medium of HUVECs.

Encapsulation of cancer cells in core-shell microcapsules

The fluids in the shell (from I2 inlet) and core (from I3 inlet) microchannels were 2% sodium alginate (purified as previously reported)[61] and neutralized rat-tail type I collagen solution with MCF-7 cancer cells (density: 5×10^6 cells/ml), respectively. In order to minimize the mixing of the aqueous core and shell solutions during microcapsule formation, the viscosity of core solution was increased by adding 1% sodium carboxymethylcellulose while keeping the final collagen concentration between 0.5–3 mg/ml. In some cases, alginate was also added to the core solution with cells to increase the stiffness of the core ECM. A 1% sodium carboxymethyl cellulose solution was used as the extraction solution (from I4 inlet), which was necessary for stable interface between oil and the aqueous extraction fluid in the extraction channel. All the solutions were sterile and buffered with 10 mM HEPES to maintain pH 7.2 before use. Further, the osmolality of all the solutions was maintained at ~300 mOsm by the addition of D-mannitol. To make mineral oil infused with aqueous calcium chloride solution for flowing in the oil channel (from I1 inlet), stable emulsion of mineral oil and 1 g/ml aqueous calcium chloride solution (volume ratio: 5:1 with the addition of 1.2% SPAN 80) was prepared by sonication for 1 min using a Branson 450 Sonifier. Solutions (except collagen that was kept at ice temperature) were injected into the microfluidic device using Harvard Apparatus (Holliston, MA, USA) Pump 11 Elite syringe pump at room temperature to generate microcapsules suspended in the oil phase and then extract them into the aqueous extraction solution. Flow rates for core, shell, oil, and extraction flows were 100 μl/hr, 250 μl/hr, 6 ml/hr, and 4 ml/hr, respectively. Oil exited the device from outlet 2 (O2). The aqueous outlet (O1) of the device was connected to a 50 ml centrifuge tube containing cell culture medium to collect the microcapsules. The collected microcapsules were further incubated at 37 °C for 30 min in a 5% CO_2 incubator to gel collagen. The encapsulated cells were further cultured for 10 days to obtain MCF-7 cell aggregates or micro-tumors (μtumors) with 1442 ± 317 MCF-7 cancer cells *per* μtumor.

Quantification of gene expression

Gene expression was quantified using quantitative reverse transcription-polymerase chain reaction (qRT-PCR). After 10 days of culture, MCF-7 μtumors were released from the core-shell microcapsules by treating them with 75 mM sodium citrate (~5 min to dissolve the alginate shell as a result of ion chelation), followed by 1000 units/ml type I collagenase (30 min at 37 °C to dissolve the collagen ECM). The cells were then washed with isotonic (by default) PBS and centrifuged. RNAs were extracted from the cells using RNeasy plus mini kit (Qiagen, Valencia, CA, USA) by following the manufacturer's instructions. Next, reverse transcription (RT) was carried out to generate complementary DNA (cDNA) using the iScript™ cDNA synthesis kit (Bio-Rad, Hercules, CA, USA) and GeneAmp 9700 PCR system. The qRT-PCR was conducted with the superfast SYBR Green mix (Bio-Rad) using a Bio-Rad CFX96 real-time PCR system. Expression of human *VIMENTIN, E-CADHERIN, AND CXCR4* were studied with human *GAPDH* being used as the housekeeping gene. Primer sequences of all the genes are given in Table S1.

Rheological characterization

Rheological measurements of the core ECM materials in the microcapsules were carried out using a 40-mm cone geometry plate (for collagen hydrogel) and 40 mm parallel plate (for collagen-alginate hydrogel) on a TA Instruments (New Castle, DE, USA) AR-1000N rheometer. Collagen-based solutions (100 μl) at different concentrations were prepared as aforementioned and placed directly on the plate on the rheometer at 4 °C. The temperature was then raised to 37 °C for 30 min to crosslink the collagen. For samples with alginate, the solution (700 μl) was placed in a PDMS mold to make a 40 mm circular hydrogel. Alginate in the samples was crosslinked by adding calcium-infused mineral oil (prepared as aforementioned) on top of the sample in the PDMS mold. After gelling the alginate for 30 min at room temperature during which the collagen was also largely gelled, the samples (after removing oil and washing with mannitol in the PDMS mold) were placed at 37 °C for 30 min to further gel the collagen. Finally, the samples were carefully placed on the plate. Stress sweeps at a constant frequency of 1 Hz were first performed to obtain the linear viscoelastic region for collecting subsequent data. Frequency sweeps were performed in the linear viscoelastic regime to determine values of the storage/elastic (G') and loss/viscous (G'') modulus. Values at 1 Hz are reported in Figure 1d.

Formation of 3D vascularized tumor in microfluidic perfusion device

After formation of MCF-7 μtumors on day 10, core-shell microcapsules were collected and the excess medium was removed by passing them through a 100-μm cell strainer. Neutralized collagen solution was prepared on ice *as per* the manufacture's instructions (using 10× PBS, 1N NaOH, and DI water). Thereafter, the collagen solution was mixed with microcapsules (with or without μtumors) and stromal cells (HUVECs and hADSCs). The final collagen concentration in the sample was 1.5 mg/ml. Volume of microcapsules was 40% of the total volume of the mixed sample. The final density of HUVECs and hADSCs in collagen solution in the sample was 10×10^6 cells/ml and 1×10^6 cell/ml, respectively. Thereafter, the sample was carefully introduced into the sample chamber of the PDMS assembly (*i.e.*, the bonded top and bottom PDMS parts) using a 100-μl positive displacement pipette. The sample volume was ~10 μl with approximately 72,000 (in ~50 μtumors or microcapsules), 60,000, 6,000 MCF-7 cancer cells, HUVECs, and hADSCs, respectively. The PDMS assembly with the sample was immediately bonded/sealed with a 0.15-mm thick rectangular (L × W: 50 × 45 mm) glass slide to form the PDMS-glass microfluidic perfusion device loaded with sample. The sample-laden device was then put in a 37 °C and 5% CO_2 humidified incubator for 30 min to gel collagen. Two holes (1 and 3, Figure S2) connected to the same reservoir channel on one side of the sample in the device were then filled with cell culture medium of 10 mm in height (~710 μl). This produces a hydrostatic pressure to drive the perfusion of the sample.[35] To initiate direct cell-cell interactions between cell in the MCF-7 μtumors and stromal cells, the sample was perfused with 75 mM sodium citrate solution for 5 min after one-day culture to dissolve the alginate shell of the microcapsules in the sample. The sample was then perfused with PBS for 5 min to remove the dissolved sodium alginate and residual sodium citrate solution, and fresh medium was added for further perfusion culture.

The samples made of the three types of single cells (hADSCs, HUVECs, and MCF-7 cells) were prepared and perfused in the same way except that single MCF-7 cells of the same amount as that in the μtumors were used. The samples for conventional static culture were prepared in the same way except that they were pipetted into the wells of 24-well plates for gelling at 37 °C in a 5% CO_2 humidified incubator for 30 min and further culturing statically in the plates with 1 ml of the same medium used for dynamic culture in the microfluidic perfusion device.

Imaging and immunostaining

Fibrous collagen ECM in the core of microcapsules was visualized using scanning electron microscopy (SEM). For SEM, the core-shell microcapsules were fixed by glutaraldehyde followed by dehydration through a series of treatments with ethanol and chemical dryer hexamethyldisilazane (HMDS). Samples were then mounted on an aluminum stub using double stick carbon tape, coated with a very thin film of Au in a sputter coater, and imaged with an FEI NOVA nano400 scanning electron microscope.

The sample in the microfluidic perfusion device was imaged every day using a Zeiss Axio Observer Z1 microscope. On day 4, samples were washed by perfusion with PBS for 5 min, and fixed by perfusion with 4% paraformaldehyde for 20 min at room temperature. After fixation, samples were washed 3 times by perfusion with PBS for 5 min, and blocked and permeabilized by perfusion with 3% bovine serum albumin (BSA) and 1% (v/v) Triton X-100 in 1× PBS buffer for 1 hr at room temperature, respectively. Following blocking, samples were incubated/perfused with rabbit polyclonal CD31 antibody (Abcam ab28364) and rabbit monoclonal VE-Cadherin antibody (Cell Signaling D87F2) at the ratio of 1:50 and 1:100, respectively, for overnight at 4 °C. Next day, the unbounded antibody was removed by washing/perfusing the samples with PBS for three times (5 min for each time). The samples were then incubated with secondary antibody at a ratio of 1:200 dilution with 1% BSA in PBS for 1 hr at room temperature. After 1 hr, excess antibody was washed 3 times by perfusion with PBS for 5 min, and the cell nuclei were stained using Hoechst. The samples were then imaged using an Olympus FV1000 spectral confocal microscope. To analyze the lumen structures in the samples, the Bitplane (Concord, MA, USA) Imaris 3D/4D image processing and analysis software (version 8.4) was used.

For immunofluorescence staining with CD44 and CD24, 2D-cultured cells, 3D avascular μtumors and 3D vascularized tumors were fixed with 4% paraformaldehyde for 20 min at room temperature. After fixation, samples were washed 3 times with PBS. After washing, samples were incubated in 3% BSA in 1× PBST at room temperature for 1 hr to block potential non-specific binding. Following that, samples were incubated overnight at 4 °C with CD44 antibody (Abcam, ab97478) at the dilution ratio of 1:100. Next day, unbounded antibody was washed with PBS for 3 times (5 min each). Then the samples were incubated with secondary antibody at the dilution ratio of 1:200 in PBS with 1% BSA at room temperature. After 1 hr, excess antibody was washed 3 times with PBS. Afterward, the samples were incubated with CD24-PE (Miltenyi Biotec Ltd., Cambridge, MA, USA) for 1 hr at room temperature. Following that, samples were washed 3 times with PBS (5 min

each), and the cell nuclei were stained using Hoechst (1 μg/ml). The samples were then imaged using an Olympus FV1000 spectral confocal microscope.

In vivo tumorigenesis and cryo-sectioning

Athymic female NU/NU nude mice (6–8 weeks old) were purchased from Charles River and were maintained on a 16:8 hr light-dark cycle. All procedures for animal usage were approved by the Institutional Animal Care and Use Committee (IACUC) at The Ohio State University and utmost care was taken to minimize suffering. To obtain xenograft model of the human mammary cancer, 3D μtumors within the microcapsules together with HUVECs and hADSCs in 1.5 mg/ml collagen solution (prepared in the same way as aforementioned for *in vitro* experiments) were injected subcutaneously in mice. A total of 100 μl of sample was injected *per* mice. After 1 day, half of the mice were injected with 75 mM sodium citrate solution at 5 different locations (20 μl per location, 100 μl in total) to dissolve the alginate shell of the microcapsules. For control experiments, ~1.4×10^6 of 2D-cultured cancer cells (equivalent to the total number of cells in 100 μl of the 3D system) or the mixture of the three types of single cells (at the same ratio as that in the 3D system and ~1.4×10^6 in total) were suspended in 100 μl of 1.5 mg/ml collagen solution and injected *per* mice. The mice were euthanized at 2 weeks after the injection. Tumors were collected, weighed, formalin fixed, paraffin embedded, and hematoxylin & eosin (H&E) stained for further histological analysis. Cryo-sections of the tumors were also prepared for immunofluorescence staining with FITC-tagged human CD31 antibody (Abcam ab13466). A total of 3 tumors (from 3 mice) were analyzed *per* group.

Preparation and characterization of drug-laden nanoparticles

The lipid (DPPC) coated fullerene (C60)-silica (S) hybrid (LC60S) nanoparticles were prepared using a reverse microemulsion method as previously reported by our group.[60] The LC60S nanoparticles were further loaded with DOX and indocyanine green (ICG) by soaking with DOX and then ICG for 30 min, respectively. The encapsulation efficiency is 98.4% and the loading content was 4.7% for both DOX and ICG. The nanoparticle size (diameter, nm) and surface zeta potential were determined using a Brookhaven (Holtsville, NY, USA) 90 Plus/BI-MAS dynamic light scattering (DLS) instrument. The morphology of nanoparticles was characterized using standard sample preparation protocols for both transmission (TEM) and scanning (SEM) electron microscopy. All the aforementioned methods for characterizing the nanoparticles are detailed in our previous publication.[60]

In vitro drug response

For drug response studies, 20,000 of 2D-cultured MCF-7 cells, hADSCs, HUVECs, or the mixture of the three types of cells (at the same ratio as that in the 3D system) were seeded in each well of 24-well plates for 12 hr before drug treatment. The attached cells had ~100% confluency with the maximum cell-cell contact to mimic the extensive cell-cell contact in the 3D MCF-7 μtumors obtained as aforementioned. For drug treatment, a total of 100 of the μtumors in core-shell microcapsules were placed in each well of 24-well plates. The 3D vascularized tumors were formed in the microfluidic perfusion device as aforementioned and treated with drug *in situ*. All the different samples were incubated/perfused for 4 days with free DOX (dissolved in culture medium) of various concentrations. Some of the 3D

vascularized tumors in the microfluidic devices were also treated/perfused with DOX and ICG-laden nanoparticles (LC60S-DI) at various concentrations in culture medium. After 12 hr of perfusion with the LC60S-DI containing medium, samples were irradiated with near infrared (NIR, 800 nm) laser at 1.5 W/cm^2 for 1 min and further cultured for 3.5 days with a total culture time of 4 days. To determine the cell viability after 4 days, all the samples were washed with PBS (3D vascularized tumors were perfused for 5 min with PBS), and fresh medium with 10% CCK-8 (Dojindo, Rockville, MD, USA) reagent was added to each sample and incubated/perfused for 4 hr at 37 °C. Afterward, 100 μl of medium/perfusate was pipetted from the samples/devices and placed in each well of a 96-well plate. Thereafter, the absorbance at 450 nm was quantified using a Perkin Elmer Victor™ X4 multilabel plate reader. Cell viability was calculated as the ratio of absorbance of each experimental sample to that of control samples cultured in pure medium for each group.

Flow cytometry analysis

For flow cytometry studies, MCF-7 aggregates were released from the core-shell microcapsules by treating them with 75 mM sodium citrate (~5 min to dissolve alginate) and then 1000 units/ml type I collagenase (30 min at 37 °C to remove the collagen ECM). The samples were then washed with PBS and centrifuged. The dissociated MCF-7 cells were washed with 1× PBS and stained with CD44-FITC (Invitrogen, Carlsbad, CA, USA) and CD24-PE (Miltenyi Biotec Ltd., Cambridge, MA, USA) antibodies according to the manufacturer's instructions. Lastly, the stained samples were analyzed using a BD LSR-II Flow Cytometer together with BD FACS Diva software (Franklin Lakes, NJ, USA).

ELISA analysis of VEGF

VEGF production was determined using ELISA (Novex™, Frederick, MD, USA) according to the manufacturer's instructions. Briefly, the 20,000 2D cultured cancer cells or the same number of cancer cells in the encapsulated 3D avascular μtumors obtained as aforementioned were cultured in 1 ml of medium in 24-well plates. A total of 100 μl of the medium was collected and the sample replenished with fresh medium every day for 4 days. For ELISA assay, 50 μl of the incubation buffer was added to all wells except that for chromogen blanks. A total of 50 μl of standard diluent buffer was mixed with 50 μl of sample or controls in the wells. Then, the preparations were incubated for 2 hr at room temperature. After adding 100 μl of human VEGF biotin conjugate solution into each well for 1 hr at room temperature, 100 μl of streptavidin-HRP was added into each well except the chromogen blanks. The plate (with plate cover) was incubated for 30 min at room temperature. Afterward, 100 μl of stabilized chromogen was added into each well. Finally, 100 μl of stop solution was added into each well to stop the reaction. The samples were then read for absorbance at 450 nm using a BioTek Synergy HT multi-detection microplate reader (Winooski, VT, USA).

Statistical analysis

All data are reported as the mean ± standard deviation of results from at least three independent runs conducted at three different times. Student's two-tailed t-test assuming equal variance was performed in Graphpad Prism (version 5, San Diego, CA, USA) to determine the p-value for assessing statistical significance ($p < 0.05$).

Supplementary Material

Refer to Web version on PubMed Central for supplementary material.

Acknowledgments

Funding Sources

This work was partially supported by grants from American Cancer Society (ACS # 120936-RSG-11-109-01-CDD) and NIH (R01CA206366).

References

1. Siegel RL, Miller KD, Jemal A. Cancer Statistics, 2016. CA Cancer J Clin. 2016; 66:7–30. [PubMed: 26742998]
2. Miller KD, Siegel RL, Lin CC, Mariotto AB, Kramer JL, Rowland JH, Stein KD, Alteri R, Jemal A. Cancer Treatment and Survivorship Statistics, 2016. CA Cancer J Clin. 2016; 66:271–289. [PubMed: 27253694]
3. Paul SM, Mytelka DS, Dunwiddie CT, Persinger CC, Munos BH, Lindborg SR, Schacht AL. How to Improve R&D Productivity: The Pharmaceutical Industry's Grand Challenge. Nat Rev Drug Discov. 2010; 9:203–214. [PubMed: 20168317]
4. Seok J, Warren HS, Cuenca AG, Mindrinos MN, Baker HV, Xu W, Richards DR, McDonald-Smith GP, Gao H, Hennessy L, Finnerty CC, Lopez CM, Honari S, Moore EE, Minei JP, Cuschieri J, Bankey PE, Johnson JL, Sperry J, Nathens AB, Billiar TR, West MA, Jeschke MG, Klein MB, Gamelli RL, Gibran NS, Brownstein BH, Miller-Graziano C, Calvano SE, Mason PH, Cobb JP, Rahme LG, Lowry SF, Maier RV, Moldawer LL, Herndon DN, Davis RW, Xiao W, Tompkins RG. Genomic Responses in Mouse Models Poorly Mimic Human Inflammatory Diseases. Proc Natl Acad Sci USA. 2013; 110:3507–3512. [PubMed: 23401516]
5. Rice J. Animal Models: Not Close Enough. Nature. 2012; 484:S9. [PubMed: 22509510]
6. van der Worp HB, Howells DW, Sena ES, Porritt MJ, Rewell S, O'Collins V, Macleod MR. Can Animal Models of Disease Reliably Inform Human Studies? PLoS Med. 2010; 7:e1000245. [PubMed: 20361020]
7. Griffith LG, Swartz MA. Capturing Complex 3d Tissue Physiology *In Vitro*. Nat Rev Mol Cell Biol. 2006; 7:211–224. [PubMed: 16496023]
8. Ridky TW, Chow JM, Wong DJ, Khavari PA. Invasive Three-Dimensional Organotypic Neoplasia from Multiple Normal Human Epithelia. Nat Med. 2010; 16:1450–1455. [PubMed: 21102459]
9. Hotary KB, Allen ED, Brooks PC, Datta NS, Long MW, Weiss SJ. Membrane Type I Matrix Metalloproteinase Usurps Tumor Growth Control Imposed by the Three-Dimensional Extracellular Matrix. Cell. 2003; 114:33–45. [PubMed: 12859896]
10. Asghar W, El Assal R, Shafiee H, Pitteri S, Paulmurugan R, Demirci U. Engineering Cancer Microenvironments for *In Vitro* 3-D Tumor Models. Mater Today. 2015; 18:539–553.
11. Villasante A, Vunjak-Novakovic G. Tissue-Engineered Models of Human Tumors for Cancer Research. Expert Opin Drug Discov. 2015; 10:257–268. [PubMed: 25662589]
12. Xu X, Farach-Carson MC, Jia X. Three-Dimensional *In Vitro* Tumor Models for Cancer Research and Drug Evaluation. Biotechnol Adv. 2014; 32:1256–1268. [PubMed: 25116894]
13. Yamada KM, Cukierman E. Modeling Tissue Morphogenesis and Cancer in 3d. Cell. 2007; 130:601–610. [PubMed: 17719539]
14. Yip D, Cho CH. A Multicellular 3d Heterospheroid Model of Liver Tumor and Stromal Cells in Collagen Gel for Anti-Cancer Drug Testing. Biochem Biophys Res Commun. 2013; 433:327–332. [PubMed: 23501105]
15. Jain RK. Normalization of Tumor Vasculature: An Emerging Concept in Antiangiogenic Therapy. Science. 2005; 307:58–62. [PubMed: 15637262]
16. Ruoslahti E. Specialization of Tumour Vasculature. Nat Rev Cancer. 2002; 2:83–90. [PubMed: 12635171]

17. Chung AS, Lee J, Ferrara N. Targeting the Tumour Vasculature: Insights from Physiological Angiogenesis. Nat Rev Cancer. 2010; 10:505–514. [PubMed: 20574450]
18. Zhang W, Zhao S, Rao W, Snyder J, Choi JK, Wang J, Khan IA, Saleh NB, Mohler PJ, Yu J, Hund TJ, Tang C, He X. A Novel Core-Shell Microcapsule for Encapsulation and 3d Culture of Embryonic Stem Cells. J Mater Chem B. 2013; 1:1002–1009.
19. Farokhzad OC, Langer R. Impact of Nanotechnology on Drug Delivery. ACS Nano. 2009; 3:16–20. [PubMed: 19206243]
20. Wang H, Yu J, Lu X, He X. Nanoparticle Systems Reduce Systemic Toxicity in Cancer Treatment. Nanomedicine (Lond). 2016; 11:103–106. [PubMed: 26653177]
21. Sykes EA, Chen J, Zheng G, Chan WC. Investigating the Impact of Nanoparticle Size on Active and Passive Tumor Targeting Efficiency. ACS Nano. 2014; 8:5696–5706. [PubMed: 24821383]
22. Fourre N, Millot JM, Garnotel R, Jeannesson P. *In Situ* Analysis of Doxorubicin Uptake and Cytotoxicity in a 3d Culture Model of Human Ht-1080 Fibrosarcoma Cells. Anticancer Res. 2006; 26:4623–4626. [PubMed: 17201187]
23. Holohan C, Van Schaeybroeck S, Longley DB, Johnston PG. Cancer Drug Resistance: An Evolving Paradigm. Nat Rev Cancer. 2013; 13:714–726. [PubMed: 24060863]
24. Meads MB, Gatenby RA, Dalton WS. Environment-Mediated Drug Resistance: A Major Contributor to Minimal Residual Disease. Nat Rev Cancer. 2009; 9:665–674. [PubMed: 19693095]
25. Morin PJ. Drug Resistance and the Microenvironment: Nature and Nurture. Drug Resist Updat. 2003; 6:169–172. [PubMed: 12962682]
26. Tredan O, Galmarini CM, Patel K, Tannock IF. Drug Resistance and the Solid Tumor Microenvironment. J Natl Cancer Inst. 2007; 99:1441–1454. [PubMed: 17895480]
27. Bersini S, Yazdi IK, Talo G, Shin SR, Moretti M, Khademhosseini A. Cell-Microenvironment Interactions and Architectures in Microvascular Systems. Biotechnol Adv. 2016; 34:1113–1130. [PubMed: 27417066]
28. Rezaei Nejad H, Goli Malekabadi Z, Kazemzadeh Narbat M, Annabi N, Mostafalu P, Tarlan F, Zhang YS, Hoorfar M, Tamayol A, Khademhosseini A. Laterally Confined Microfluidic Patterning of Cells for Engineering Spatially Defined Vascularization. Small. 2016; 12:5132–5139. [PubMed: 27510763]
29. Jeon JS, Bersini S, Gilardi M, Dubini G, Charest JL, Moretti M, Kamm RD. Human 3d Vascularized Organotypic Microfluidic Assays to Study Breast Cancer Cell Extravasation. Proc Natl Acad Sci US A. 2015; 112:214–219.
30. Chiu LL, Montgomery M, Liang Y, Liu H, Radisic M. Perfusable Branching Microvessel Bed for Vascularization of Engineered Tissues. Proc Natl Acad Sci US A. 2012; 109:E3414–3423.
31. Wang X, Phan DT, Sobrino A, George SC, Hughes CC, Lee AP. Engineering Anastomosis between Living Capillary Networks and Endothelial Cell-Lined Microfluidic Channels. Lab Chip. 2016; 16:282–290. [PubMed: 26616908]
32. Moya ML, Hsu YH, Lee AP, Hughes CC, George SC. *In Vitro* Perfused Human Capillary Networks. Tissue Eng Part C Methods. 2013; 19:730–737. [PubMed: 23320912]
33. Hsu YH, Moya ML, Hughes CC, George SC, Lee AP. A Microfluidic Platform for Generating Large-Scale Nearly Identical Human Microphysiological Vascularized Tissue Arrays. Lab Chip. 2013; 13:2990–2998. [PubMed: 23723013]
34. Baranski JD, Chaturvedi RR, Stevens KR, Eyckmans J, Carvalho B, Solorzano RD, Yang MT, Miller JS, Bhatia SN, Chen CS. Geometric Control of Vascular Networks to Enhance Engineered Tissue Integration and Function. Proc Natl Acad Sci US A. 2013; 110:7586–7591.
35. Chan JM, Zervantonakis IK, Rimchala T, Polacheck WJ, Whisler J, Kamm RD. Engineering of *In Vitro* 3D Capillary Beds by Self-Directed Angiogenic Sprouting. PLoS One. 2012; 7:e50582. [PubMed: 23226527]
36. Kim C, Kasuya J, Jeon J, Chung S, Kamm RD. A Quantitative Microfluidic Angiogenesis Screen for Studying Anti-Angiogenic Therapeutic Drugs. Lab Chip. 2015; 15:301–310. [PubMed: 25370780]

37. Bischel LL, Young EW, Mader BR, Beebe DJ. Tubeless Microfluidic Angiogenesis Assay with Three-Dimensional Endothelial-Lined Microvessels. Biomaterials. 2013; 34:1471–1477. [PubMed: 23191982]
38. Zheng Y, Chen J, Craven M, Choi NW, Totorica S, Diaz-Santana A, Kermani P, Hempstead B, Fischbach-Teschl C, Lopez JA, Stroock AD. *In Vitro* Microvessels for the Study of Angiogenesis and Thrombosis. Proc Natl Acad Sci US A. 2012; 109:9342–9347.
39. Song JW, Munn LL. Fluid Forces Control Endothelial Sprouting. Proc Natl Acad Sci US A. 2011; 108:15342–15347.
40. Song JW, Bazou D, Munn LL. Anastomosis of Endothelial Sprouts Forms New Vessels in a Tissue Analogue of Angiogenesis. Integr Biol. 2012; 4:857–862.
41. Lee VK, Kim DY, Ngo H, Lee Y, Seo L, Yoo SS, Vincent PA, Dai G. Creating Perfused Functional Vascular Channels Using 3d Bio-Printing Technology. Biomaterials. 2014; 35:8092–8102. [PubMed: 24965886]
42. Zorlutuna P, Annabi N, Camci-Unal G, Nikkhah M, Cha JM, Nichol JW, Manbachi A, Bae H, Chen S, Khademhosseini A. Microfabricated Biomaterials for Engineering 3d Tissues. Adv Mater. 2012; 24:1782–1804. [PubMed: 22410857]
43. Castells M, Thibault B, Delord JP, Couderc B. Implication of Tumor Microenvironment in Chemoresistance: Tumor-Associated Stromal Cells Protect Tumor Cells from Cell Death. Int J Mol Sci. 2012; 13:9545–9571. [PubMed: 22949815]
44. Shi Y, Du L, Lin L, Wang Y. Tumour-Associated Mesenchymal Stem/Stromal Cells: Emerging Therapeutic Targets. Nat Rev Drug Discov. 2017; 16:35–52. [PubMed: 27811929]
45. Acerbi I, Cassereau L, Dean I, Shi Q, Au A, Park C, Chen YY, Liphardt J, Hwang ES, Weaver VM. Human Breast Cancer Invasion and Aggression Correlates with Ecm Stiffening and Immune Cell Infiltration. Integr Biol. 2015; 7:1120–1134.
46. Chen L, Xiao Z, Meng Y, Zhao Y, Han J, Su G, Chen B, Dai J. The Enhancement of Cancer Stem Cell Properties of Mcf-7 Cells in 3d Collagen Scaffolds for Modeling of Cancer and Anti-Cancer Drugs. Biomaterials. 2012; 33:1437–1444. [PubMed: 22078807]
47. Levental KR, Yu H, Kass L, Lakins JN, Egeblad M, Erler JT, Fong SF, Csiszar K, Giaccia A, Weninger W, Yamauchi M, Gasser DL, Weaver VM. Matrix Crosslinking Forces Tumor Progression by Enhancing Integrin Signaling. Cell. 2009; 139:891–906. [PubMed: 19931152]
48. Chaudhuri O, Koshy ST, Branco da Cunha C, Shin JW, Verbeke CS, Allison KH, Mooney DJ. Extracellular Matrix Stiffness and Composition Jointly Regulate the Induction of Malignant Phenotypes in Mammary Epithelium. Nat Mater. 2014; 13:970–978. [PubMed: 24930031]
49. Weaver VM, Petersen OW, Wang F, Larabell CA, Briand P, Damsky C, Bissell MJ. Reversion of the Malignant Phenotype of Human Breast Cells in Three-Dimensional Culture and *In Vivo* by Integrin Blocking Antibodies. J Cell Biol. 1997; 137:231–245. [PubMed: 9105051]
50. Chandler EM, Seo BR, Califano JP, Andresen Eguiluz RC, Lee JS, Yoon CJ, Tims DT, Wang JX, Cheng L, Mohanan S, Buckley MR, Cohen I, Nikitin AY, Williams RM, Gourdon D, Reinhart-King CA, Fischbach C. Implanted Adipose Progenitor Cells as Physicochemical Regulators of Breast Cancer. Proc Natl Acad Sci US A. 2012; 109:9786–9791.
51. Barcellos-de-Souza P, Gori V, Bambi F, Chiarugi P. Tumor Microenvironment: Bone Marrow-Mesenchymal Stem Cells as Key Players. Biochim Biophys Acta. 2013; 1836:321–335. [PubMed: 24183942]
52. Mandel K, Yang Y, Schambach A, Glage S, Otte A, Hass R. Mesenchymal Stem Cells Directly Interact with Breast Cancer Cells and Promote Tumor Cell Growth *In Vitro* and *In Vivo*. Stem Cells Dev. 2013; 22:3114–3127. [PubMed: 23895436]
53. Fischbach C, Kong HJ, Hsiong SX, Evangelista MB, Yuen W, Mooney DJ. Cancer Cell Angiogenic Capability Is Regulated by 3d Culture and Integrin Engagement. Proc Natl Acad Sci US A. 2009; 106:399–404.
54. Zhang W, Choi JK, He X. Engineering Microvascularized 3d Tissue Using Alginate-Chitosan Microcapsules. J Biomater Tissue Eng. 2016; 7:170–173.
55. Rao W, Wang H, Han J, Zhao S, Dumbleton J, Agarwal P, Zhang W, Zhao G, Yu J, Zynger DL, Lu X, He X. Chitosan-Decorated Doxorubicin-Encapsulated Nanoparticle Targets and Eliminates

Tumor Reinitiating Cancer Stem-Like Cells. ACS Nano. 2015; 9:5725–5740. [PubMed: 26004286]

56. Wang H, Agarwal P, Zhao S, Xu RX, Yu J, Lu X, He X. Hyaluronic Acid-Decorated Dual Responsive Nanoparticles of Pluronic F127, Plga, and Chitosan for Targeted Co-Delivery of Doxorubicin and Irinotecan to Eliminate Cancer Stem-Like Cells. Biomaterials. 2015; 72:74–89. [PubMed: 26344365]
57. Gilbert CA, Ross AH. Cancer Stem Cells: Cell Culture, Markers, and Targets for New Therapies. J Cell Biochem. 2009; 108:1031–1038. [PubMed: 19760641]
58. Chin AR, Wang SE. Cytokines Driving Breast Cancer Stemness. Mol Cell Endocrinol. 2014; 382:598–602. [PubMed: 23562748]
59. Korkaya H, Liu S, Wicha MS. Breast Cancer Stem Cells, Cytokine Networks, and the Tumor Microenvironment. J Clin Invest. 2011; 121:3804–3809. [PubMed: 21965337]
60. Wang H, Agarwal P, Zhao S, Yu J, Lu X, He X. A Biomimetic Hybrid Nanoplatform for Encapsulation and Precisely Controlled Delivery of Theranostic Agents. Nat Commun. 2015; 6:10081. [PubMed: 26621191]
61. Choi JK, Agarwal P, Huang H, Zhao S, He X. The Crucial Role of Mechanical Heterogeneity in Regulating Follicle Development and Ovulation with Engineered Ovarian Microtissue. Biomaterials. 2014; 35:5122–5128. [PubMed: 24702961]

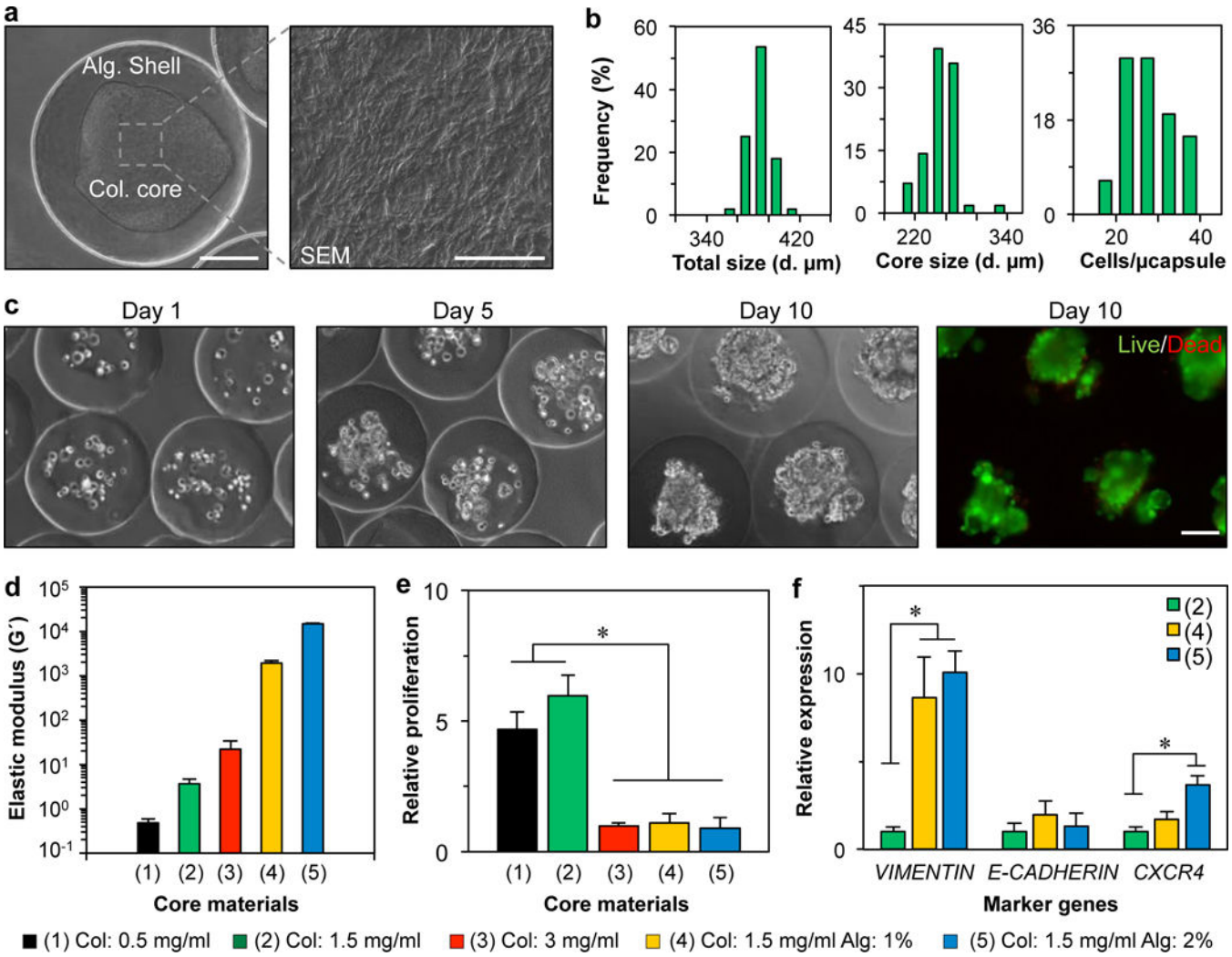

Figure 1.

Characterization of proliferation and gene expression of avascular 3D μtumors. (**a**) A differential interference contrast (DIC) image of a typical microcapsule showing its core-shell morphology and a scanning electron microscopy (SEM) image showing collagen (1.5 mg/ml) fibers in the microcapsule core. Alg: alginate and Col: collagen. (**b**) Distribution of the total and core size of the microcapsules together with the distribution of the number of cells in them. (**c**) Typical phase contrast and fluorescence (live/dead) images of the encapsulated cells in microcapsules with a 1.5 mg/ml collagen core, showing the cell proliferation over 10 days. (**d**) Elastic modulus of different core ECMs. (**e**) Quantification of relative cell proliferation represented by the size of aggregates on day 10 obtained from culturing the cells in different collagen core ECMs in the microcapsules. The size is normalized to that of the 3 mg/ml collagen core condition. (**f**) Quantitative RT-PCR data showing the effect of matrix stiffness on the expression of mesenchymal (*VIMENTIN* and *CXCR4*) and epithelial (*E-CADHERIN*) phenotype markers of cells in the μtumors. The symbol * denotes $p < 0.05$. Scale bar: (a) 100 μm for the DIC image or 5 μm for the SEM image and (c) 100 μm.

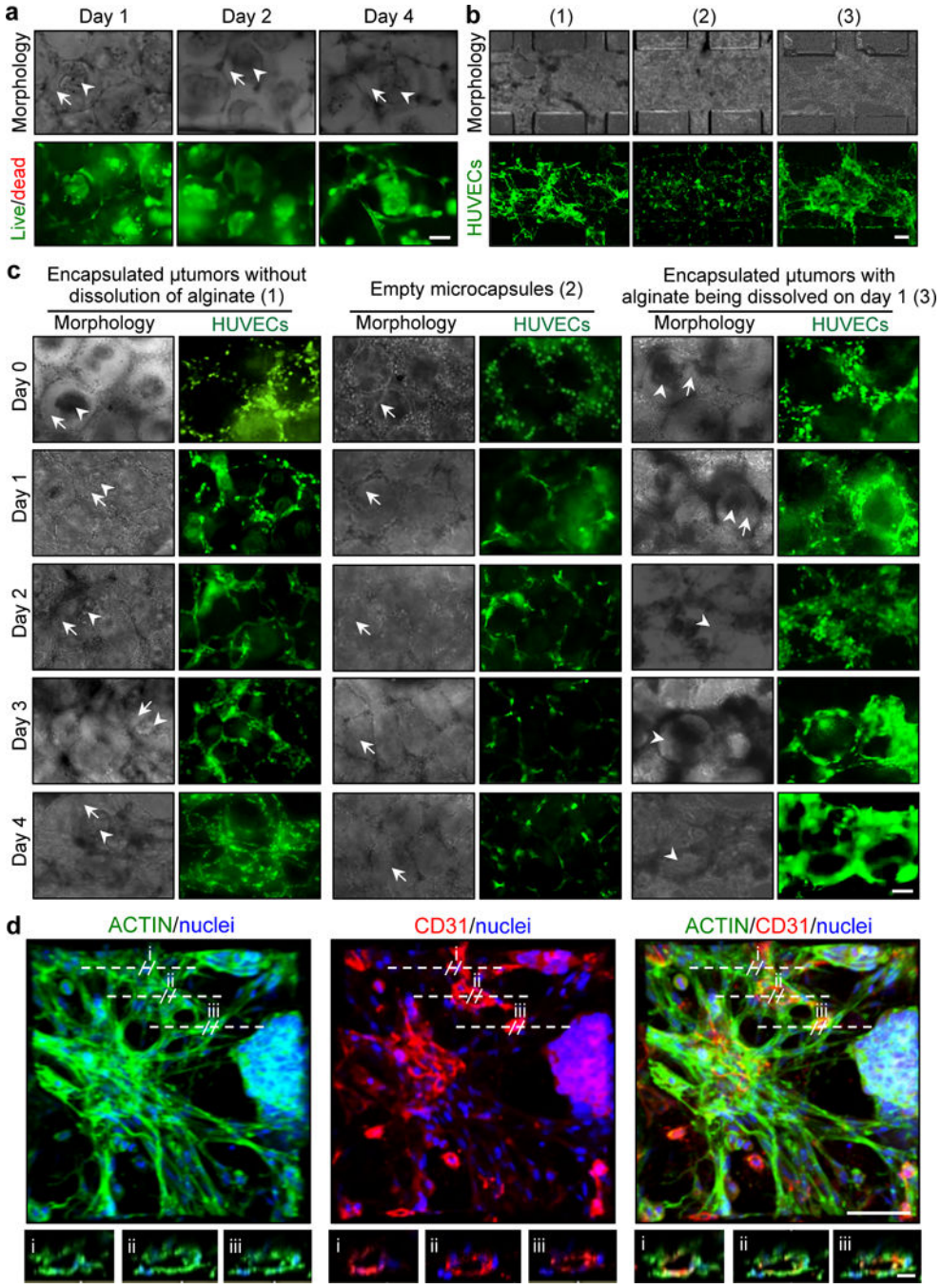

Figure 2.

Assembly of μtumors in the microfluidic perfusion device to form vascularized 3D tumor. (**a**) Live/dead staining of the vascularized tumor on different days showing high cell viability. HUVECs without green fluorescence protein (GFP) were used. Arrow and arrowhead represent microcapsule shell and μtumor, respectively. (**b**) Phase contrast and fluorescence images (4×) showing vessel formation on day 4 with (1) μtumors encapsulated in microcapsules, (2) empty microcapsules, and (3) μtumors without microcapsules (the alginate hydrogel shell was dissolved by perfusing the samples with 75 mM sodium citrate

solution for 5 min after one day of culturing the sample). HUVECs with GFP were used. (**c**) Time-lapse micrographs at 10× showing the progression of vessel formation within 4 days. Extensive vascularization was observed on days 3 and 4 when the μtumors were present, whereas vascularization was minimal with empty microcapsules. Moreover, removing the alginate hydrogel shell after one-day culture further facilitates vascularization. Arrow and arrowhead represent microcapsule shell and μtumor, respectively. (**d**) The vessel structure visualized by staining for ACTIN filament, CD31, and cell nuclei. Cross-sectional images (i, ii, and iii) demonstrate the presence of lumen in the vessels. HUVECs without GFP were used. Scale bar: (a and c) 100 μm, (b) 200 μm, (d) 50 μm and for cross-sectional images: 20 μm.

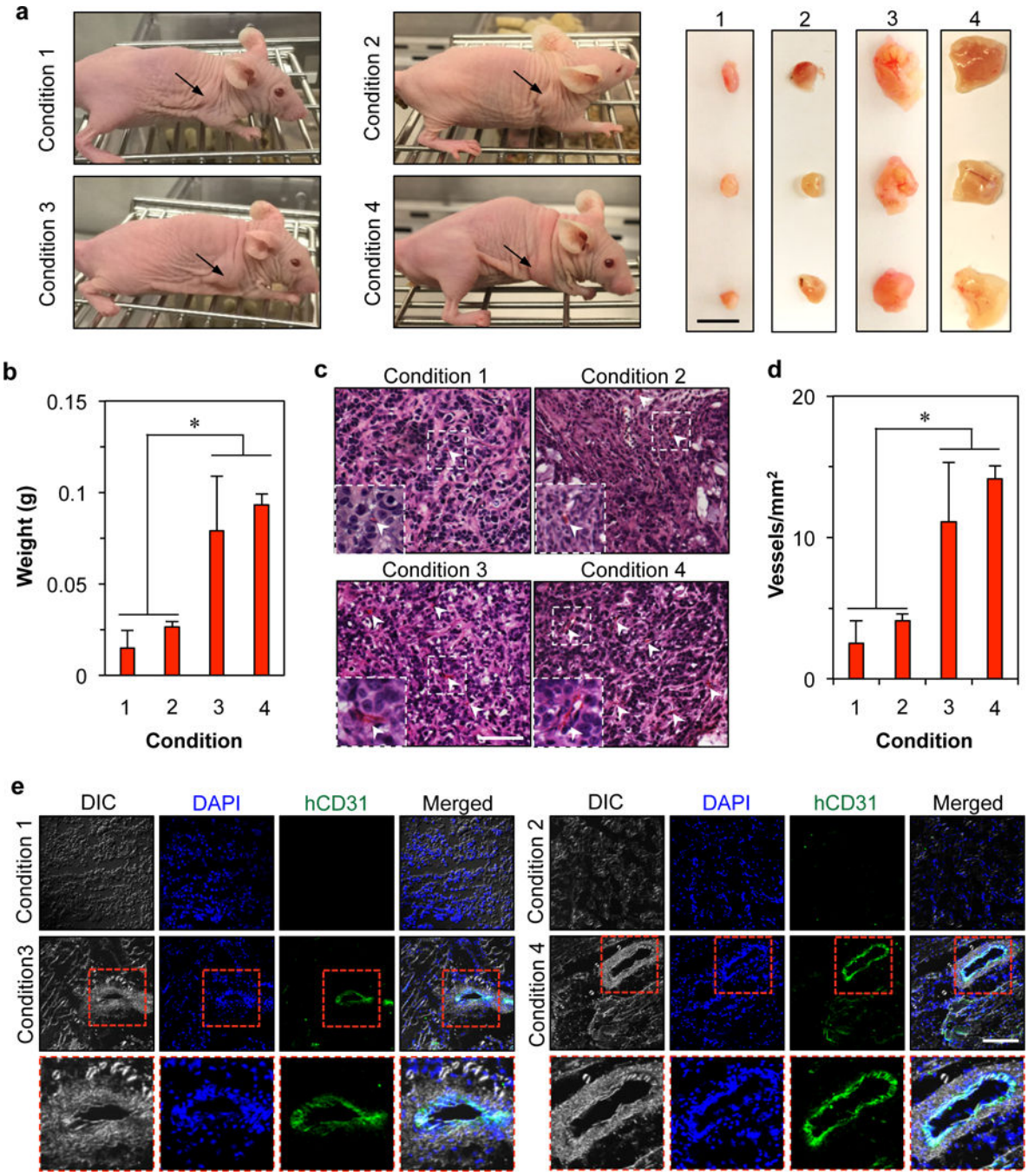

Figure 3.

In vivo tumorigenicity of the 3D-engineered system of encapsulated μtumors, HUVECs, and hADSCs in collagen. (**a**) Photographs of mice and tumors obtained on 14 days after subcutaneously injecting single 2D-cultured MCF-7 cancer cells aone (condition 1), mixture of single hADSCs, HUVEC, 2D-cultured MCF-7 cancer cells (condition 2), the 3D-engineered system (condition 3), and the 3D-engineered system with dissolution of alginate at 1 day after injection (condition 4) in collagen into athymic nude mice. The total number of cells were the same for all the conditions. (**b**) Weight of the tumors collected on day 14

post subcutaneous injection. (**c**) Representative histology (H&E) images of tumors, showing blood vessels with red blood cells (RBCs, arrow heads). (**d**) Quantitative measurement of the density of blood vessels in tumors obtained from the four conditions. (**e**) Confocal images of immunofluorescent staining for human CD31 (hCD31, green) and cell nuclei (blue) in the tumors. HUVECs without GFP were used. The symbol * denotes $p < 0.05$. Scale bar: (a) 5 mm, (c) 40 μm, (e) 100 μm.

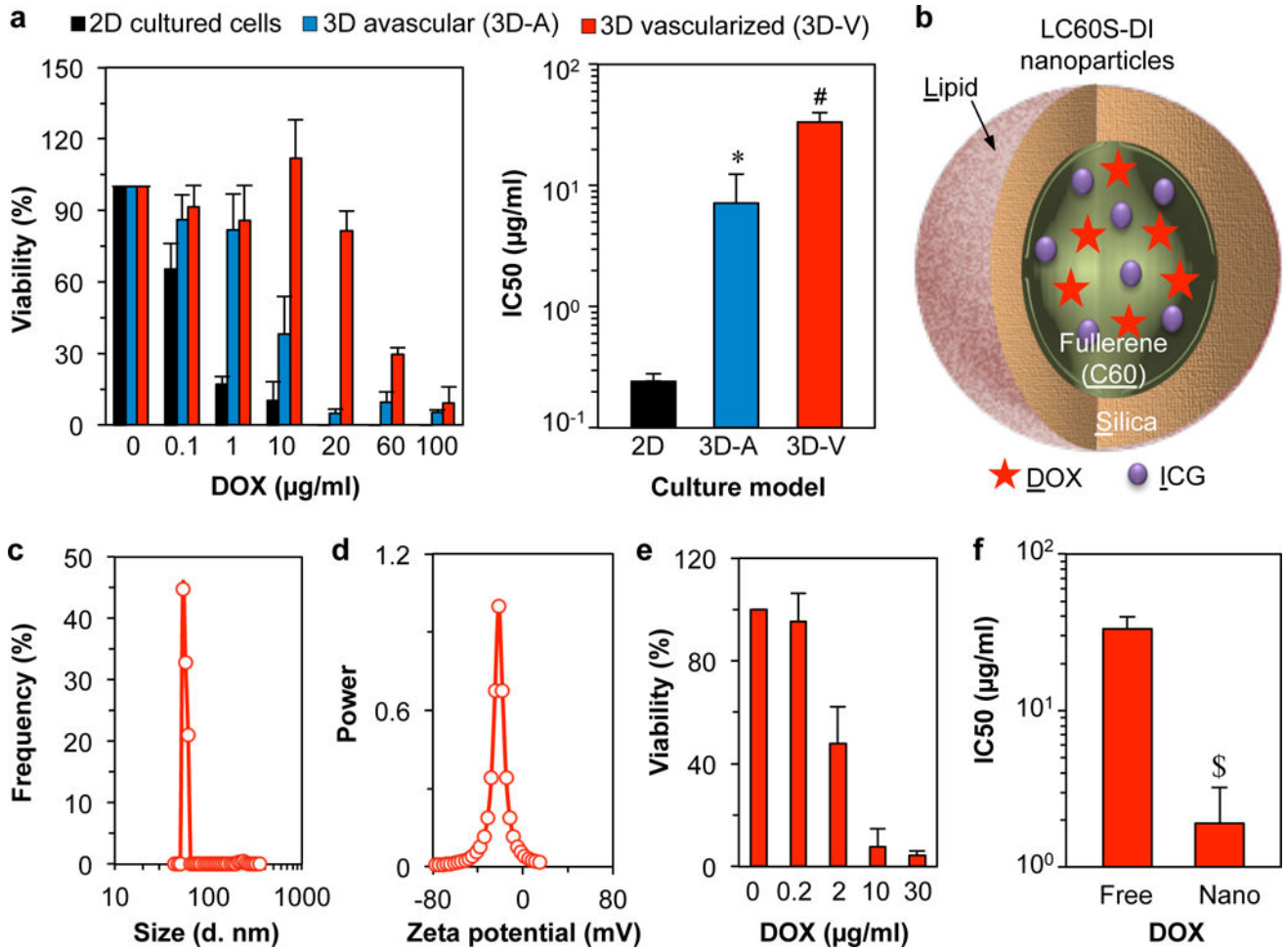

Figure 4.

Drug response of the 3D vascularized tumor. (**a**) Viability of 2D-cultured cancer cells, 3D avascular μtumors (3D-A), and 3D vascularized tumors (3D-V) after 4 days of incubation or treatment with free doxorubicin hydrochloride (DOX). Also shown is the IC50 of free DOX for the three different tumor models. The symbol * denotes $p < 0.05$ when compared to 2D-cultured cancer cells, and # denotes $p < 0.05$ when compared with 2D-cultured cancer cells and 3D avascular μtumors. (**b**) A schematic illustration of the LC60S-DI nanoparticles consisting of lipid (L), fullerence (C60), silica (S), DOX (D) and indocyanine green (ICG or I). (**c**) Size distribution and (**d**) surafce zeta potential of the nanoparticles determined by dynamic light scattering (DLS). (**e**) Viability of all cells in 3D-V after 4 days of treatment with LC60S-DI with various effective DOX concentrations. (**f**) IC50 of free and nanoencapsulated DOX for the destruction of 3D vascularized tumors. The symbol $ denotes $p < 0.05$ when comparing between the free and nanoparticle-encapsulated DOX.

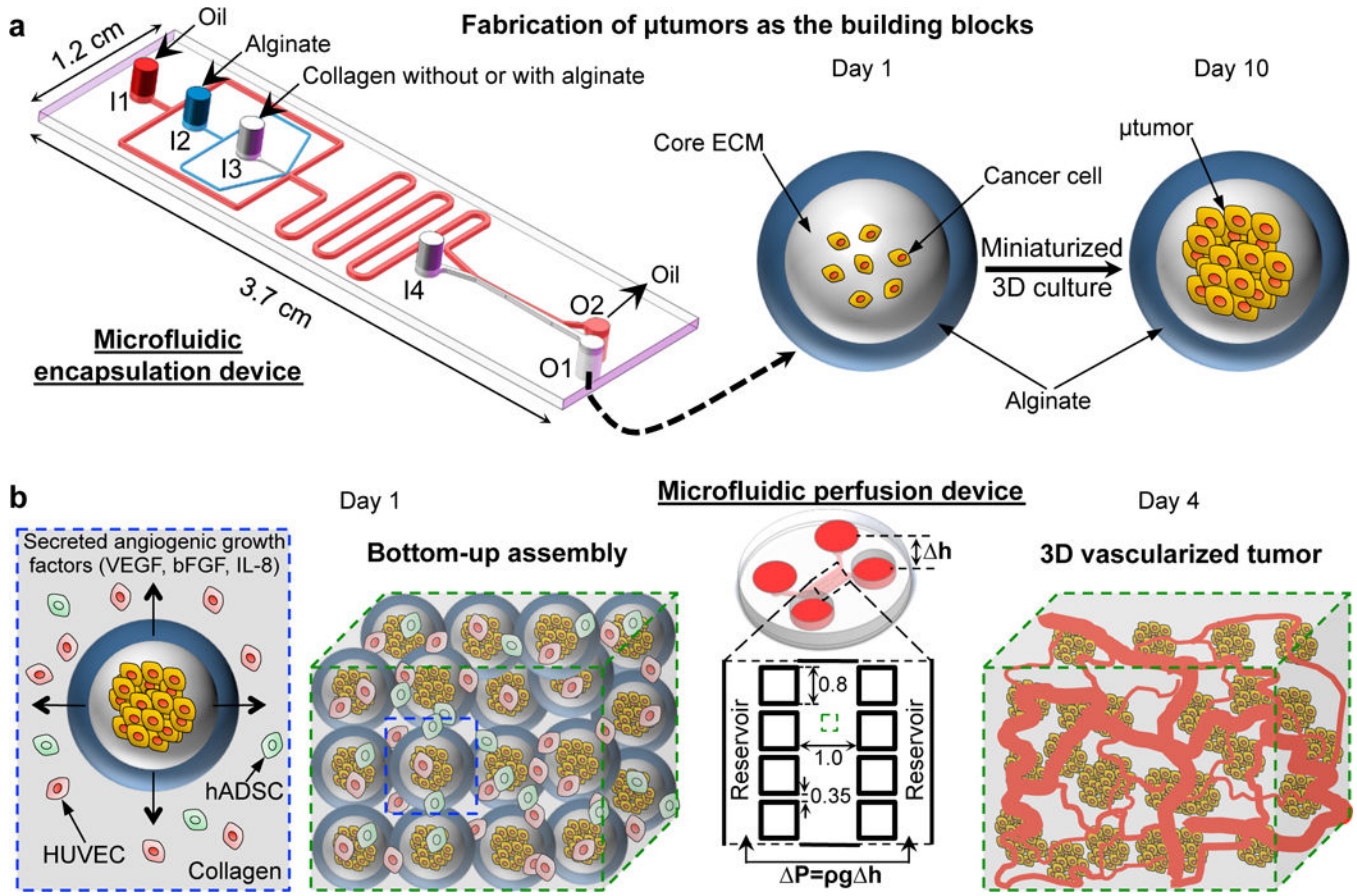

Scheme 1.

Schematic illustration of the bottom-up approach for creating 3D vascularized human tumor. (**a**) A non-planar microfluidic encapsulation device is used for encapsulating cancer cells in core-shell microcapsules and the cells are cultured in the microcapsules for 10 days to form micro-tumors (µtumors, less than ~200 µm in radius). Mineral oil infused with calcium chloride, aqueous sodium alginate solution (to form the microcapsule shell), aqueous collagen solution (with or without cells) to form the microcapsule core, and aqueous extraction solution are pumped into the device *via* inlets I1, I2, I3, and I4, respectively. The aqueous phase (containing core-shell microcapsules) and oil exit the device from outlets O1 and O2, respectively. (**b**) A microfluidic perfusion device is used to assemble the µtumors and stromal cells including endothelial cells for perfusion culture to form 3D vascularized tumor. The µtumors in core-shell microcapsules are assembled together with human umbilical vein endothelial cells (HUVECs) and human adipose-derived stem cells (hADSCs) in collagen hydrogel in the microfluidic perfusion device. The alginate shell of the microcapsules is dissolved to allow cell-cell interactions and the formation of 3D vascularized tumor in the microfluidic perfusion device under perfusion driven by hydrostatic pressure. Unit for the dimensions of micro-pillars and sample chamber: mm; P: pressure; ρ: density; g: gravitational acceleration; and h: height of medium column linked to the reserviors.